Mediterranean Archaeology and Archaeometry, Vol. 10, No. 4, pp. 43-51

ESTABLISHING A CHRONOLOGY FOR LANDSCAPE EVOLUTION AROUND A FINAL PALAEOLITHIC SITE AT ARENDONK-*KORHAAN* (NE BELGIUM): FIRST RESULTS FROM OPTICALLY STIMULATED LUMINESCENCE DATING

C. Derese[1], D.A.G. Vandenberghe[1], M. van Gils[2,3], B. Vanmontfort[3], E. Meirsman[3], F. Mees[4], P. van den Haute[1]

[1]Laboratory of Mineralogy and Petrology (Luminescence Research Group), Department of Geology and Soil Science, Ghent University, Krijgslaan 281 (S8), B-9000 Gent, Belgium

[2]Flemish Heritage Institute, Phoenix Building, Koning Albert II-laan 19, Bus 5, B-1210 Brussel, Belgium

[3]Prehistorical Archaeology Unit, Katholieke Universiteit Leuven, Celestijnenlaan 200E, PB 2409, B-3001 Heverlee, Belgium

[4]Royal Museum for Central Africa, Leuvensesteenweg 13, B-3080 Tervuren, Belgium

Corresponding author: Cilia.Derese@UGent.be

ABSTRACT

Optically stimulated luminescence (OSL) dating was applied to constrain the timing of aeolian activity and surface stability around the Final Palaeolithic site at Arendonk-*Korhaan*. The sequence under investigation consists of coversands and an intercalated bleached horizon, which is thought to represent the Usselo Soil of Allerød age. This horizon contains a concentration of lithics that can be attributed to the Final Palaeolithic *Federmesser* culture.

All samples show satisfactory luminescence characteristics. While the equivalent doses and dose rates show an unexpected spread, the resulting optical ages are internally consistent and in agreement with geological and archaeological expectations. The coversands under- and overlying the bleached horizon are dated at 14.2 ± 1.1 ka (n = 5) and 11.7 ± 0.9 ka (n = 2), respectively; the horizon itself yields an age of 14.1 ± 1.3 ka. As such, the results allow distinguishing two discrete phases of aeolian deposition, and they confirm that the intercalated bleached horizon represents the Usselo Soil of Allerød age. It is concluded that, throughout the Late Glacial, the site was only fit for human occupation during the milder climatic and environmental conditions of the Allerød stage.

KEYWORDS: optically stimulated luminescence; quartz; Final Palaeolithic; coversand; Late Glacial; Usselo Soil; *Federmesser*

INTRODUCTION

In the coversand area of NE Belgium, the earliest traces of human presence after the Weichselian Last Glacial Maximum (LGM) are located in the Usselo Soil of Allerød age (13.0 – 14.0 ka calBP; Hoek, 2001), which is a widespread marker horizon in the Late Glacial sandy sequences that are spread all over N Europe (Kaiser et al., 2009). The traces mainly consist of lithic artefacts, which, based on their technological and typological characteristics, are attributed to the Final Palaeolithic *Federmesser-gruppen*. The *Federmessergruppen* mainly occupied open-air sites and presumably had a nomadic lifestyle (De Bie and Vermeersch, 1998); this way of life made them vulnerable to changing climatic and environmental conditions.

As to why the *Federmesser* tradition disappeared from the area, remains to be established. It might relate to the abrupt and drastic environmental and climatic changes at the Allerød/Late Dryas transition, such as extensive forest fires, severe cooling-down and re-intensification of aeolian activity (De Bie and Vermeersch, 1998). It is clear that gaining insight into the environmental settings of *Federmesser* sites will improve our knowledge on the rise, development and fall of the culture. This requires a reliable chronological framework for the landscape evolution and environmental change around the archaeological sites.

The objective of the present study is to establish a chronology for coversand accumulation at the *Federmesser* site of Arendonk-*Korhaan* using the optically stimulated luminescence dating method. This research is part of a more extensive study that aims at establishing a solid chronological framework for the evolution of climate and landscape around some of the most important Final Palaeolithic settlements in the NW European lowlands.

GEOLOGICAL SETTING AND PROFILE DESCRIPTION

The investigated site at Arendonk-*Korhaan* (Fig. 1a) is located in the Campine lowland plain (NE Belgium). It forms part of an extensive site complex, known as Landschap De Liereman-*Duinengordel*, which is located on the border between the municipalities of Oud-Turnhout and Arendonk. The investigated profile is situated on an elongated NE-SW oriented coversand ridge (locally known as "*De Korhaan*"), which defines the southernmost border of a larger ridge system (Fig. 1b). A swampy depression is present south of the ridge (Meirsman et al., 2008).

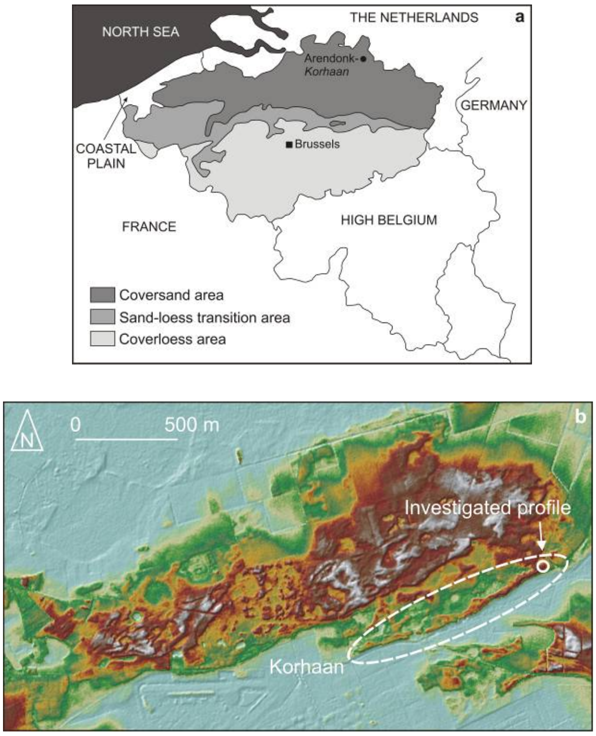

Fig. 1: (a) Schematic map of Belgium, showing the main aeolian sedimentation areas and the location of the investigated site (filled circle); (b) Digital elevation map of the coversand ridge complex and the archaeological site Landschap De Liereman – *Duinengordel*. The coversand ridge "*Korhaan*" is marked with a dashed line, the location of the investigated profile with an open circle. Elevated areas are shown in brown and white (highest), the depression areas in green and light blue (lowest).

In this study, one profile near the ridge crest has been investigated (Fig. 2); it is described in detail by Meirsman et al. (2008). The profile shows a sedimentary sequence of about 1.5 m, which consists of coversands intercalated by a bleached horizon and capped by a podzol. The lowermost unit, with an average thickness of ~50 cm in the profile, is made up of alternating layers of coarse- and fine-grained sands with an oblique stratification; the layers probably represent the prograding slip face of the coversand ridge. This unit is capped by horizontally layered sands with a thickness of 5-10 cm, separated from the overlying sands by a 10-20 cm thick bleached horizon with similar sedimentary characteristics. This bleached horizon follows the relief of the coversand ridge and laterally grades into a peat layer close to the depression. Meirsman et al. (2008) distinguish two subunits within this layer: (1) a white sandy unit, and (2) a light grey slightly loamy unit, in which most of the Final Palaeolithic artefacts are concentrated. The bleached layer is covered by 60-70 cm of yellow-coloured aeolian sands with a more massive bedding. A ~30 cm thick podzol has developed in the top of this sandy unit; this podzol is partly disturbed by ploughing marks.

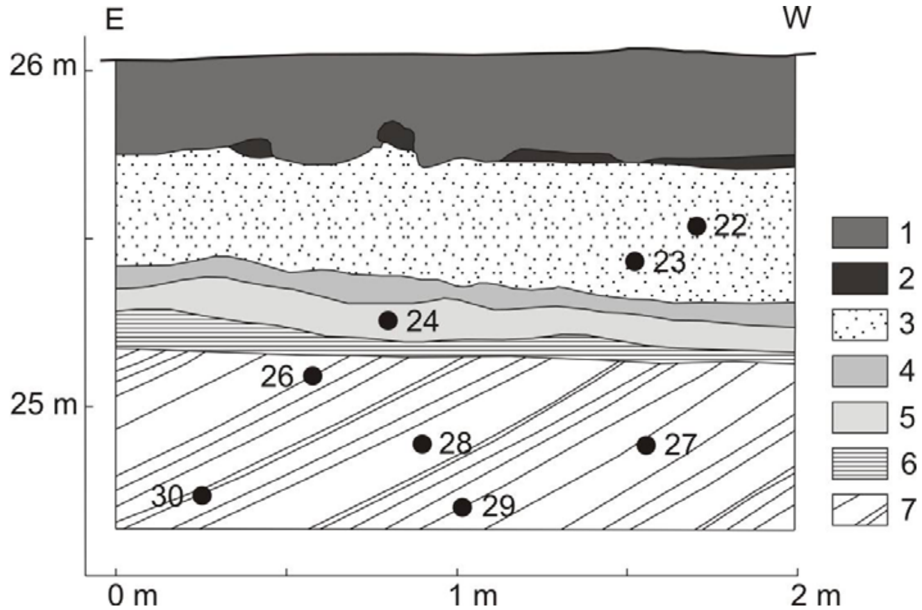

Fig. 2: Schematic representation of the sampled profile (adapted from Meirsman et al., 2008). 1: podzol, 2: illuviation horizon of podzol, 3: Younger Coversand II, 4: silty part of Usselo horizon, 5: sandy part of Usselo horizon, 6: horizontally stratified Younger Coversand I, 7: obliquely stratified Younger Coversand I. The location of the samples for luminescence dating is indicated with filled circles.

Based on the stratigraphic position and lithological characteristics of the bleached horizon and on the intercalated archaeological finds, this layer is thought to be equivalent to the Usselo Soil of Allerød age (13.0 – 14.0 ka calBP). This interpretation is corroborated by optical dating results that were previously obtained in another profile on the coversand ridge. In this profile, situated about 25 m to the west of the profile investigated here, ages of 14.5 ± 1.1 ka and 14.8 ± 1.2 ka were obtained for two samples taken below the Usselo Soil (Vandenberghe, 2005). Based on their stratigraphical position under- and overlying the Usselo Soil, the sandy deposits can be interpreted as the equivalents of the Older Coversands II and/or Younger Coversands I, and the Younger Coversands II, respectively (Meirsman et al., 2008), which are assumed to be deposited from the final phase of the Late Pleniglacial onwards and during the Late Glacial (Kasse et al., 2007).

SAMPLING, SAMPLE PREPARATION AND ANALYTICAL FACILITIES

Eight samples for OSL dating were collected by gently hammering stainless steel cylinders into the freshly cleaned sediment exposure. A high-resolution sampling strategy was adopted, with multiple samples being taken from each sediment unit; one sample was collected from the intercalated bleached horizon (Fig. 2). About 1 kg of the surrounding sediment was collected for laboratory dose rate determination. Three undisturbed sediment samples (one per sedimentary unit) were taken for evaluation of the time-averaged water content.

Coarse (180-212 μm) quartz grains were extracted from the inner cores of the sampling tubes in the conventional manner (HCl, H_2O_2, sieving, HF). The purity of the quartz extracts was confirmed by the absence of a significant infrared stimulated luminescence (IRSL) response at 60°C to a large (~50 Gy) regenerative beta dose. The sensitivity to infrared was defined as significant if the resulting signal amounted to more than 10% of the corresponding OSL signal (Vandenberghe, 2004) or if the IR depletion ratio deviated more than 10% from unity (Duller, 2003). All OSL measurements were performed in an automated Risø TL/OSL-DA-12 reader, equipped with blue (470 ± 30 nm) LEDs and an IR laser diode (830 nm). The quartz luminescence emissions were detected through 7.5 mm of Hoya U-340 UV filter. Details on the measurement apparatus can be found in Bøtter-Jensen et al. (2003).

Determination of the dose rate was based on low-level gamma-ray spectrometry in the laboratory. The sediment was oven dried (at 110°C until constant weight), homogenised and pulverised. A subsample of ~140 g was subsequently cast in wax and stored for one month before being measured on top of the detector. Details on the experimental setup, spectrum evaluation and radionuclide concentration calculation can be found in Vandenberghe (2004) and De Corte et al. (2006).

EQUIVALENT DOSE DETERMINATION

Equivalent doses were determined using the single-aliquot regenerative-dose (SAR) protocol (Murray and Wintle, 2000). Optical stimulation with blue LEDs was for 40 s at 125°C; a preheat of 240°C for 10 s and a test dose cutheat to 160°C were adopted. After the measurement of each test dose signal, a high-temperature bleach was performed by stimulation with the blue diodes for 40 s at 280°C (Murray and Wintle, 2003). The initial 0.32 s of the decay curve minus a background integrated between 1.44 and 2.08 s was used in all calculations. In all samples, the quartz OSL signal is dominated by the fast component (Fig. 3, inset). The dose-response curves can be well represented by single saturating exponential functions (Fig. 3); recycling ratios are close to unity and recuperation values are low (<0.5%). This illustrates the generally good behaviour of the samples in the SAR protocol.

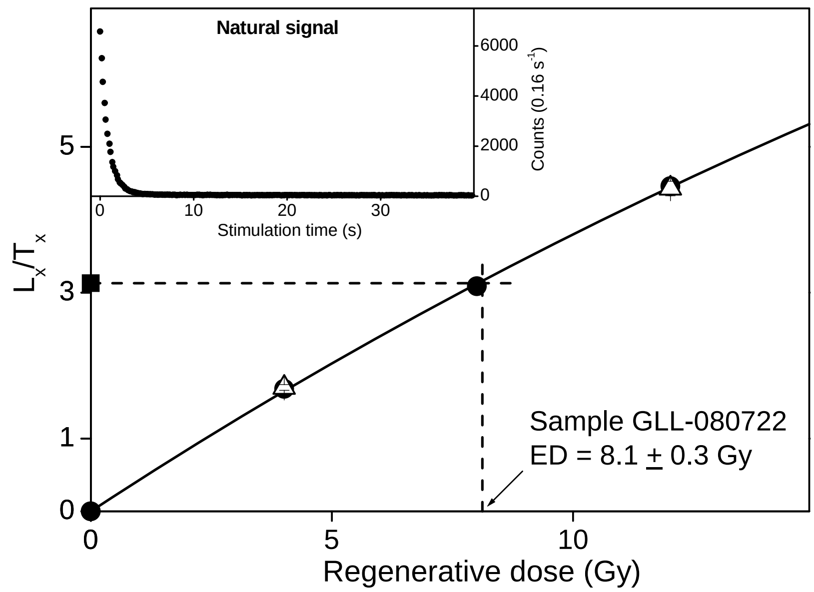

Fig. 3: Illustrative dose-response curve and natural OSL decay curve (inset) for an aliquot of 180-212 µm quartz grains extracted from sample GLL-080722. The solid line is the fit of the data to a single saturated exponential function. The open triangles represent recycling points. The equivalent dose (ED) is obtained by interpolation of the sensitivity-corrected natural OSL signal (filled square) on the corrected growth curve.

A dose recovery test was carried out, in which three natural aliquots of each sample were bleached using the blue diodes at room temperature (2 times 250 s, with a 10 ks pause in between), and given a laboratory dose close to the expected natural dose before any heat treatment was applied. For each sample, the measured dose does not differ from the given dose by more than 10% and the overall average measured to given dose ratio is 1.05 ± 0.01 (n = 24); the corresponding overall average recycling ratio is 0.98 ± 0.01, while the recuperated signal amounts to 0.21 ± 0.03% of the sensitivity-corrected natural OSL signal. The results from the dose recovery tests indicate that the SAR protocol is able to measure laboratory doses given prior to any heat treatment with reasonable accuracy.

For each sample, 18 replicate measurements of the equivalent dose were made. The average values (± 1 standard error) are summarised in Fig. 4a and Table 1. The equivalent doses show no clear increase with depth, and show a relatively large spread throughout the profile. This spread is unexpected, for a number of reasons: (1) both sediment units consist of a very similar and rather homogeneous body of quartz-rich sand, so that the dose rate is not expected to vary significantly throughout the profile (or at least within each unit); (2) several studies indicate that aeolian sandy sediments in the NW European lowlands have been well-bleached (Derese et al., 2009; Vandenberghe, 2004; Vandenberghe et al., 2003; 2009); (3) there are no macroscopic indications for large-scale post-depositional disturbance (such as bioturbation) of the investigated profile.

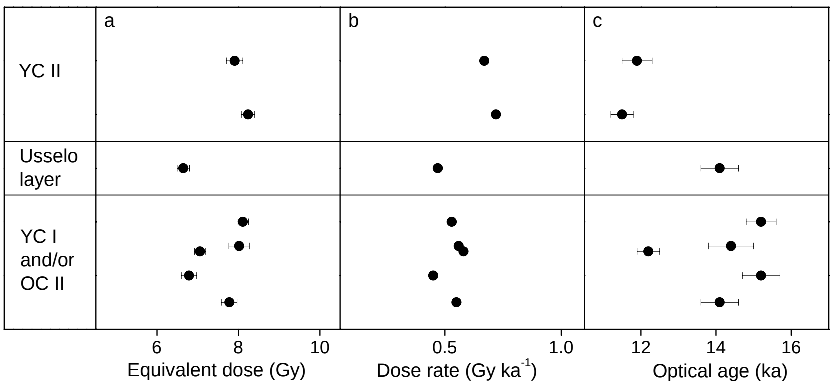

Fig. 4: Plot of the (a) equivalent doses, (b) dose rates, and (c) resulting optical ages as a function of the stratigraphic position of the samples (not on scale). The error bars represent the random uncertainty (1σ) only.

Table 1: Summary of the radionuclide activities, estimated time-averaged moisture contents, calculated dose rates, equivalent doses (D_e), optical ages, and random (σ_r), systematic (σ_{sys}) and total (σ_{tot}) uncertainties. The uncertainties mentioned with the dosimetry and De data are random; all uncertainties represent 1σ. All sources of systematic uncertainty were assessed following Vandenberghe (2004; see also Vandenberghe et al, 2004). The uncertainties were propagated following the error assessment system as outlined in Aitken (1985, appendix B).

Sample GLL-code	Depth (cm)	^{234}Th (Bq kg^{-1})	^{226}Ra (Bq kg^{-1})	^{210}Pb (Bq kg^{-1})	^{232}Th (Bq kg^{-1})	^{40}K (Bq kg^{-1})	Water Content (%)	Total Dose rate (Gy ka^{-1})	D_e (Gy)	Age (ka)	σ_r (%)	σ_{sys} (%)	σ_{tot} (%)	σ_{tot} (ka)
080722	57	4.5 ± 0.5	5.9 ± 0.1	5.6 ± 0.8	5.0 ± 0.1	89 ± 2	5 ± 1	0.67 ± 0.01	7.9 ± 0.2	11.9	3.2	7.8	8.4	1.0
080723	67	5.8 ± 1.2	6.8 ± 0.2	6.9 ± 0.9	5.2 ± 0.2	99 ± 2	5 ± 1	0.72 ± 0.01	8.2 ± 0.2	11.5	2.8	7.8	8.3	0.9
080724	80	3.4 ± 0.7	3.3 ± 0.2	3.1 ± 0.8	2.6 ± 0.1	54 ± 2	4 ± 1	0.47 ± 0.01	6.7 ± 0.2	14.1	3.7	8.2	9.0	1.3
080725	97	3.7 ± 0.7	4.8 ± 0.2	5.1 ± 0.8	3.7 ± 0.2	64 ± 1	6 ± 2	0.53 ± 0.01	8.1 ± 0.1	15.2	2.9	7.4	8.0	1.2
080728	116	5.2 ± 0.8	5.6 ± 0.4	4.7 ± 0.7	4.0 ± 0.1	72 ± 2	6 ± 2	0.56 ± 0.01	8.0 ± 0.3	14.4	3.8	7.3	8.2	1.2
080727	118	5.5 ± 0.8	5.4 ± 0.2	4.8 ± 0.6	4.0 ± 0.1	79 ± 2	6 ± 2	0.58 ± 0.01	7.1 ± 0.1	12.2	2.7	7.2	7.7	0.9
080726	129	4.2 ± 0.7	4.0 ± 0.2	3.4 ± 0.6	3.1 ± 0.2	49 ± 1	6 ± 2	0.45 ± 0.01	6.8 ± 0.2	15.2	3.6	7.7	8.5	1.3
080729	135	5.3 ± 0.7	4.9 ± 0.1	4.9 ± 0.9	4.0 ± 0.1	72 ± 1	6 ± 2	0.55 ± 0.01	7.8 ± 0.2	14.1	3.5	7.3	8.1	1.1

DOSE RATE DETERMINATION

The dosimetric information is summarised in Table 1. Radionuclide activity concentrations were converted to dose rates using factors derived from the nuclear energy releases tabulated by Adamiec and Aitken (1998). A factor of 0.9 (± 5% relative uncertainty) was adopted to correct the external beta dose rates for the effects of attenuation and etching (Mejdahl, 1979). An internal dose rate in quartz grains of 0.010 ± 0.002 Gy/ka was assumed (Vandenberghe et al., 2008). The evaluation of the time-averaged moisture content, and the corresponding correction for it of the dose rates, was performed following the procedure outlined in Aitken (1985). The time-averaged moisture content was chosen to be equal to the present-day moisture content (~4-6%); a much higher water percentage is unlikely due to the location of the site and the nature of the sediments. An increase in the water content of 1% results in an equal increase in the optical age. The contribution from cosmic radiation was calculated following Prescott and Hutton (1994) and a relative systematic uncertainty of 15% was associated with this value.

The total dose rates are relatively low, due to the quartz-rich nature of the sediments; the values range from ~0.4 to ~0.7 Gy ka^{-1}, and the variation throughout the profile (Fig. 4b) broadly matches the pattern observed for the equivalent doses (Fig. 4a). The dose rates for the sediment unit overlying the bleached horizons (samples GLL-080722 and -23) are somewhat higher than the values for the horizon itself as well as for the underlying sediments (~0.7 Gy ka^{-1} vs ~0.5-0.6 Gy ka^{-1}). It remains to be established whether or not this originates with podzolisation in the overlying unit. However, we observed no disequilibrium in the ^{238}U series and the activity concentrations of all measured radionuclides are higher (Table 1); it thus seems unlikely that preferential post-depositional redistribution of radionuclides has affected the dose rate of this uppermost sediment unit. As the total dose rate is dominated by contributions from cosmic rays and ^{40}K (both ~30-40%), minor variations in ^{238}U daughter activity concentrations are not expected to lead to significant uncertainties in the age determination.

OPTICAL AGE DETERMINATION

Table 1 summarises all the information relevant to the age and uncertainty calculation. In Fig. 4c, the optical ages are plotted according to the stratigraphic position of the samples. As the sources of systematic uncertainty (e.g. source calibration, conversion factors, cosmic radiation, internal radioactivity) are largely shared between the samples, only the random uncertainty (~3 – 4%) is considered to evaluate the internal consistency of the ages. Within this uncertainty, the age results are generally in agreement with the stratigraphic position of the samples; the dataset for each sediment unit shows no increase with depth. One sample from the deposits underlying the bleached horizon (sample GLL-080727) yields an age of 12.2 ± 0.3 ka (1 random uncertainty), which appears significantly younger than the other dates obtained for this unit (~14-15 ka). Assuming that the set of ages reflects a single depositional event (within the limit on the time-resolution that can be achieved using OSL dating), the Q test (Dean and Dixon, 1951) was used to test whether this value represents an outlier; it was found that the date of 12.2 ± 0.3 ka is not significantly different from the other values at the 95% confidence level. This variability illustrates the importance of obtaining several age estimates for a single sedimentary unit.

An average optical age of 14.2 ± 1.1 ka (n = 5) was obtained for the sediment unit underlying the bleached horizon, while the overlying unit is dated at 11.7 ± 0.9 ka (n = 2); the sample from the bleached horizon yields an age of 14.1 ± 1.3 ka. These dates are in agreement with the expected Late Glacial age of the profile, which is based on the interpretation of the archaeological finds (lithics of the *Federmessergruppen*) in a horizon that on stratigraphic grounds was thought to represent the Usselo Soil of Allerød age (13.0 – 14.0 ka calBP; Hoek, 2001). Moreover, the dates for the lowermost sediment unit (14.2 ± 1.1 ka, on average) are consistent with the two optical ages of 14.5 ± 1.1 ka and 14.8 ± 1.2 ka that were previously obtained on an equivalent profile at Arendonk-*Korhaan* (Vandenberghe, 2005).

DISCUSSION AND CONCLUSIONS

The optical ages confirm that the bleached horizon represents the Usselo Soil of Allerød age, and point at two discrete aeolian phases.

A first phase is dated at 14.2 ± 1.1 ka (n = 5). It cannot be established whether the corresponding aeolian unit is equivalent to the Younger Coversand I and/or the Older Coversand II; the Lower Loamy Bed of presumed Bølling age - which is a diagnostic horizon that separates the two units in the classic lithostratigraphical record (Kasse, 2002) - is not observed. However, the optical ages for this unit range from 12.2 ± 0.9 ka to 15.2 ± 1.3 ka. This may indicate that, despite the climatic improvement, aeolian deposition continued from the Late Pleniglacial into the Late Glacial, as previously pointed out by Kasse et al. (2007). The aeolian activity resulted in the development of a coversand ridge complex. The progradation of the ridges is clearly visible in the profile at Arendonk-*Korhaan* as the oblique stratification that characterises the sediment unit underlying the Usselo Soil (Fig. 2).

The Younger Coversand I / Older Coversand II unit is capped by the Usselo Soil, of which the sedimentary component is dated at 14.1 ± 1.3 ka. It reflects a period of land surface stability during the Allerød interstadial, in which the increase in temperature and humidity caused vegetation growth and soil formation. The overall amelioration of the climate allowed *Federmesser* groups to migrate into the NW European lowlands. At Arendonk-*Korhaan*, they built an open-air settlement under the lee of the flank of the coversand ridge, and in the immediate vicinity of water. The top of the Usselo Soil contains charcoal, as has been observed at many localities (Hoek and Bohncke, 2002). The widespread occurrence of charcoal fragments in this stratigraphic position suggests that they are related to environmental and/or climate conditions prevailing at the onset of the Late Dryas, which caused vegetation to burn down over large areas.

The Usselo Soil is overlain by a unit of aeolian sands, which have been dated at 11.7 ± 0.9 ka (n = 2). This date, in combination with the presence of the Usselo Soil, distinguishes this aeolian phase from the previous one. These results strongly support the existence of clearly defined aeolian phases, which was previously doubted by Koster (2005). The sediment unit is equivalent to the Younger Coversand II that is normally attributed to the Late Dryas stadial. The deposits reflect a phase of landscape instability caused by climatic cooling, increased aridity, and the resulting decline of the vegetation cover.

As the Younger Coversand II unit contains no traces of occupation, it is concluded that *Federmesser* groups had already disappeared from the area at about 11.7 ± 0.9 ka. The changes in climate and environment at the end of the Allerød and throughout the Late Dryas may have turned the coversand ridge complex (and the Campine region in general) into an inhospitable place, which led the nomads to make tracks and never return.

This study illustrates that optical dating provides a powerful tool for establishing a chronological framework for the environmental context of archaeological sites in the West European lowlands. Very often, it is the only method that can be applied as material suitable for radiocarbon dating is either lacking, or does not directly relate to the actual evolution of the landscape. The availability of a reliable timeframe contributes significantly to an improved understanding of how regional climatic evolution and environmental change may have influenced human occupation and cultural development.

Further optical dating studies at other Final Palaeolithic sites in the NW European lowlands, in combination with micromorphological, sedimentological and palynological analyses, are underway.

This will improve our understanding of how the Late Glacial sequences should be correlated and will allow more detailed investigations into the possible relationship between Late Glacial environmental and climatic changes, and human occupation patterns.

ACKNOWLEDGEMENTS

Luminescence research at Ghent University is financially supported by the Special Research Fund of the Ghent University (CD) and by the Research Foundation – Flanders (FWO-Vlaanderen; DV: Postdoctoral Fellow). Gilles Velghe is gratefully acknowledged for technical assistance. The participants of the 1st L.A.I.S. Symposium (9-12th of September 2009, Delphi, Greece) are thanked for stimulating discussions.

REFERENCES

Adamiec, G., Aitken, M.J., 1998. Dose-rate conversion factors: update. Ancient TL 16: 37-50.

Aitken, M.J., 1985. Thermoluminescence dating. Academic Press Inc., London. 359 pp.

Bøtter-Jensen, L., Andersen, C.E., Duller, G.A.T., Murray, A.S., 2003. Developments in radiation, stimulation and observation facilities in luminescence measurements. Radiation Measurements 37, 535-541.

De Bie, M., Vermeersch, P.M., 1998. Pleistocene-Holocene transition in Benelux. Quaternary International 49/50, 29-43.

De Corte, F., Vandenberghe, D., De Wispelaere, A., Buylaert, J.-P., Van den haute, P., 2006. Radon loss from encapsulated sediments in Ge gamma-ray spectrometry for the annual radiation dose determination in luminescence dating. Czech Journal of Physics 56, D183-D194.

Derese, C., Vandenberghe, D., Paulissen, E., Van den haute, P., 2009. Revisiting a type locality for Late Glacial aeolian sand deposition in NW Europe: Optical dating of the dune complex at Opgrimbie (NE Belgium). Geomorphology 109, 27-35.

Dean, R.B., Dixon, W.J., 1951. Simplified statistics for small numbers of observations. Analytical Chemistry 23, 636-638.

Duller, G.A.T., 2003. Distinguishing quartz and feldspar in single grain luminescence measurements. Radiation Measurements 37, 161-165.

Hoek, W.Z., 2001. Vegetation response to the ~14.7 and ~11.5 ka cal.BP climate transitions: is vegetation lagging climate? Global and Planetary Change 30, 103-115.

Hoek, W.Z., Bohncke, S.J.P., 2002. Climatic and environmental events over the Last Termination, as recorded in The Netherlands: a review. Netherlands Journal of Geosciences/Geologie en Mijnbouw 81, 123-137.

Kaiser K., Hilgers A., Schlaak N., Jankowski M., Kühn P., Bussemer S., Przegiętka K., 2009. Palaeopedological marker horizons in northern central Europe: characteristics of lateglacial Usselo and Finow soils. Boreas 38, 59-609.

Kasse, C., 2002. Sandy aeolian deposits and environments and their relation to climate during the Last Glacial Maximum and Lateglacial in northwest and central Europe. Progress in Physical Geography 26, 507-532.

Kasse, C., Vandenberghe, D., De Corte, F., Van den haute, P., 2007. Late Weichselian fluvio-aeolian sands and coversands of the type locality Grubbenvorst (southern Netherlands): sedimentary environments, climate record and age. Journal of Quaternary Science 22, 695-708.

Koster, E.A., 2005. Recent advances in luminescence dating of Late Pleistocene (cold-climate) aeolian sands and loess deposits in western Europe. Permafrost and Periglacial Processes 16, 131 – 143.

Meirsman, E., Van Gils, M., Vanmontfort, B., Paulissen, E., Bastiaens, J., Van Peer, P., 2008. Landschap De Liereman herbezocht. De waardering van een gestratifieerd finaalpaleolithisch en mesolithisch sitecomplex in de Noorderkempen (gem. Oud-Turnhout en Arendonk), Notae Praehistoricae 28, 33-41.

Mejdahl, V., 1979. Thermoluminescence dating: beta-dose attenuation in quartz grains. Archaeometry 21, 61-72.

Murray, A.S., Wintle, A.G., 2000. Luminescence dating of quartz using an improved single-aliquot regenerative-dose protocol. Radiation Measurements 32, 57-73.

Murray, A.S., Wintle, A.G., 2003. The single aliquot regenerative dose protocol: potential for improvements in reliability. Radiation Measurements 37, 377-381.

Prescott, J.R., Hutton, J.T., 1994. Cosmic ray contributions to dose rates for luminescence and ESR dating: large depths and long-term time variations. Radiation Measurements 23, 497-500.

Vandenberghe, D., 2004. Investigation of the optically stimulated luminescence dating method for application to young geological samples. Ph.D. thesis, Universiteit Gent: 358 pp.

Vandenberghe, D., 2005. Optical dating of sediments. Analysis Report GLL-001/04. Gent, Belgium.

Vandenberghe, D., Hossain, S.M., De Corte, F., Van den haute, P., 2003. Investigations on the origin of the equivalent dose distribution in a Dutch coversand. Radiation Measurements 37, 433-439.

Vandenberghe, D., De Corte, F., Buylaert, J.-P., Kučera, J., Van den haute, P., 2008. On the internal radioactivity in quartz. Radiation Measurements 43, 771-775.

Vandenberghe, D., Kasse, C., Hossain, S.M., De Corte, F., Van den haute, P., Fuchs, M., Murray, A.S., 2004. Exploring the method of optical dating and comparison of optical and ^{14}C ages of Late Weichselian coversands in the southern Netherlands. Journal of Quaternary Science 19, 73-86.

Vandenberghe, D., Vanneste, K., Verbeeck, K., Paulissen, E., Buylaert, J.-P., De Corte, F., Van den haute, P., 2009. Late Weichselian and Holocene earthquake events along the Geleen fault in NE Belgium: OSL age constraints. Quaternary International 199, 56-74.